Bioorganic & Medicinal Chemistry Letters xxx (2014) xxx–xxx

Contents lists available at ScienceDirect

Bioorganic & Medicinal Chemistry Letters

journal homepage: www.elsevier.com/locate/bmcl

Rational design of the first difluorostatone-based PfSUB1 inhibitors

Simone Giovani [a,b,c], Maria Penzo [d], Simone Brogi [a,b,c], Margherita Brindisi [a,b,c], Sandra Gemma [a,b,c,*], Ettore Novellino [a,e], Luisa Savini [a,b,c], Michael J. Blackman [d], Giuseppe Campiani [a,b,c,*], Stefania Butini [a,b,c]

[a] European Research Centre for Drug Discovery and Development (NatSynDrugs), University of Siena, via Aldo Moro 2, 53100 Siena, Italy
[b] Dip. di Biotecnologie, Chimica e Farmacia, University of Siena, via Aldo Moro 2, 53100 Siena, Italy
[c] Centro Interuniversitario di Ricerche sulla Malaria (CIRM), University of Perugia, Perugia, Italy
[d] Division of Parasitology, MRC National Institute for Medical Research, Mill Hill, London NW7 1AA, UK
[e] Dip. di Farmacia, University of Naples Federico II, Via D. Montesano 49, 80131 Naples, Italy

ARTICLE INFO

Article history:
Received 28 March 2014
Revised 12 May 2014
Accepted 13 May 2014
Available online xxxx

Keywords:
Malaria
PfSUB1
Serine protease
Difluorostatone
Egress

ABSTRACT

The etiological agent of the most dangerous form of malaria, *Plasmodium falciparum*, has developed resistance or reduced sensitivity to the majority of the drugs available to treat this deadly disease. Innovative antimalarial therapies are therefore urgently required. *P. falciparum* serine protease subtilisin-like protease 1 (PfSUB1) has been identified as a key enzyme for merozoite egress from red blood cells and invasion. We present herein the rational design, synthesis, and biological evaluation of novel and potent difluorostatone-based inhibitors. Our bioinformatic-driven studies resulted in the identification of compounds **1a**, **b** as potent and selective PfSUB1 inhibitors. The enzyme/inhibitor interaction pattern herein proposed will pave the way to the future optimization of this class of promising enzyme inhibitors.

Malaria is a plague that mainly afflicts the populations of low-income countries located in tropical and subtropical areas of the world. According to WHO data, malaria kills around 660,000 people and causes 203 million new infections each year.[1] Despite recent increases in total funding allocated by public and private organizations, the elimination of malaria remains a distant goal.[2] One of the main obstacles to malaria eradication is the emergence of strains of *Plasmodium falciparum*—the etiological agent of the most virulent form of malaria—that are resistant to existing antimalarial chemotherapeutics.[3] Artemisinin-based combination therapy (ACT) is a therapeutic regimen useful for the treatment of drug resistant *P. falciparum* strains and is characterized by low liability of selecting drug resistant parasites. The implementation of ACTs, coupled to appropriate preventive measures, raised some optimism within the scientific community towards effective control of the disease. However, this enthusiasm has been lowered by recent reports of reduced sensitivity of *P. falciparum* strains to ACTs.[4] In the face of this worrying scenario, the identification of new drugs with innovative mechanisms of action emerges as one means to effectively combat infection and parasite resistance.[5] In recent years a number of small molecules arising from phenotypic screens or directed against novel targets have entered the drug discovery and development pipelines. However, no antimalarial drugs with truly new mechanisms of action have been introduced into therapy recently.[5]

Proteases represent a broad class of drug targets that has been widely exploited for the development of chemotherapeutics useful for the treatment of a number of metabolic and/or infectious diseases. Among the various classes of proteases, only recently have serine proteases been fully exploited for their potential as drug targets.[6,7] Several proteases of *P. falciparum* have been identified as potential therapeutic targets. Among them, the serine protease *P. falciparum* subtilisin-like protease 1 (PfSUB1) has emerged as a key enzyme playing a critical role in two essential steps of the life cycle of *P. falciparum*: egress and invasion.[8–11] The lifecycle of *P. falciparum* involves a mosquito and a human stage of development. The human stage can be in turn divided into an asymptomatic exo-erythrocytic phase and a symptomatic asexual erythrocytic phase.

During this latter phase, the parasite invades and multiplies within red blood cells (RBCs), passing through successive developmental forms known as ring, trophozoite, and schizont stages. Eventual segmentation of the schizont produces 16–32 mature merozoites. Upon rupture of the RBC, the merozoites escape in a process known as egress, and invade new RBCs.[8] Egress is an active, highly regulated event involving rupture of both the parasitophorous vacuole (PV) membrane (that encloses the parasite within the RBC) and the RBC membrane.[8] The timing of egress is critical for parasite survival since premature egress of non-segmented

* Corresponding authors. Tel.: +39 0577 234326; fax: +39 0577 234254 (S.G.); tel.: +39 0577 234172; fax: +39 0577 234254 (G.C.).
E-mail addresses: gemma@unisi.it (S. Gemma), campiani@unisi.it (G. Campiani).

http://dx.doi.org/10.1016/j.bmcl.2014.05.044
0960-894X/

schizonts or immature merozoites is fatal for the parasite.[11] PfSUB1 is released in the PV space just prior to egress where it mediates the proteolytic maturation of a family of PV proteins called SERA.[10] Moreover, PfSUB1 processes several merozoite surface proteins (MSP1, MSP6, and MSP7) thus priming the merozoite for the subsequent invasion step.[9] Inhibition of PfSUB1 activity or discharge prevents SERA maturation and blocks egress and the resulting merozoites are defective in invasion.[10,11] These studies convincingly point to PfSUB1 as a promising drug target to be validated for the development of innovative antimalarial therapies.

To date, few PfSUB1 inhibitors have been described by us and others.[10,12–14] Poor potency, lack of selectivity, or poor cell permeability are the main issues in most cases. Covalent peptidyl α-ketoamide inhibitors based on authentic substrates of the protease have also been recently described.[13] With the aim of developing more potent and selective PfSUB1 inhibitors we started with the generation of a homology model of the enzyme. Very recently, during the revision of the manuscript, the PfSUB1-prodomain-NIMP.M7 Fab complex has been released, PDB ID: 4LVN.[15] Originally, to rationally design the novel inhibitors we analyzed the binding mode of the decapeptide KITAQ↓DDEES, derived from the cleavage sequence of the PfSUB1 substrate SERA4st1 (details concerning our rational design based on the homology model was provided in Supplementary data; Figs. S1–S13). Notably, acidic amino acids are present at the prime-side of all PfSUB1 cleavage sequences identified so far.[13,16] In earlier predictions[13,16] and our model, the P1′ aspartate of the decapeptide was predicted to form an interaction with the PfSUB1 residue K465. Our inhibitor design approach consisted of maintaining the natural P-side sequence of the decapeptide, whilst replacing the cleavable peptide bond with an electrophilic carbonyl group. In order to reproduce in our inhibitor the key interaction between the carboxylic function of the P1′ residue and K465, a difluorostatone moiety was envisaged as having the appropriate length to project an N-terminal carboxylic group toward K465. Fine-tuning of the distance between the electrophilic carbonyl group and the N-terminal carboxylic moiety was accomplished through the synthesis of both **1a** and **2**, differing in the length of the linker. Once we established the optimal size of the linker, the molecular weight of inhibitor **1a** was progressively reduced by eliminating amino acid residues at the P-side (Scheme 1).

The synthesis of PfSUB1 inhibitors **1a–c** and **2** is described in Scheme 2. Enantiomerically pure[17] aldehyde **4** was obtained from the commercially available Boc-protected amino acid **3** via $LiAlH_4$-mediated reduction of a *N*,*O*-dimethylhydroxamide (Weinreb amide) intermediate. Formation of the Weinreb amide was accomplished in quantitative yield by coupling **3** and *N*,*O*-dimethylhydroxylamine in the presence of 1-ethyl-3-(3-dimethylaminopropyl)carbodiimide (EDC) and hydroxybenzotriazole (HOBt). Aldehyde **4** was submitted to the Reformatsky reaction protocol using ethyl bromodifluoroacetate and activated zinc in refluxing THF to furnish alcohol **5** as a mixture of diastereoisomers.[18,19] Ethyl ester **5** was hydrolyzed with a 0.25 N solution

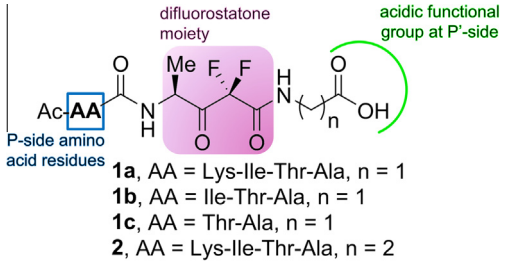

Scheme 1. Difluorostatone-based inhibitors **1a–c**, **2**.

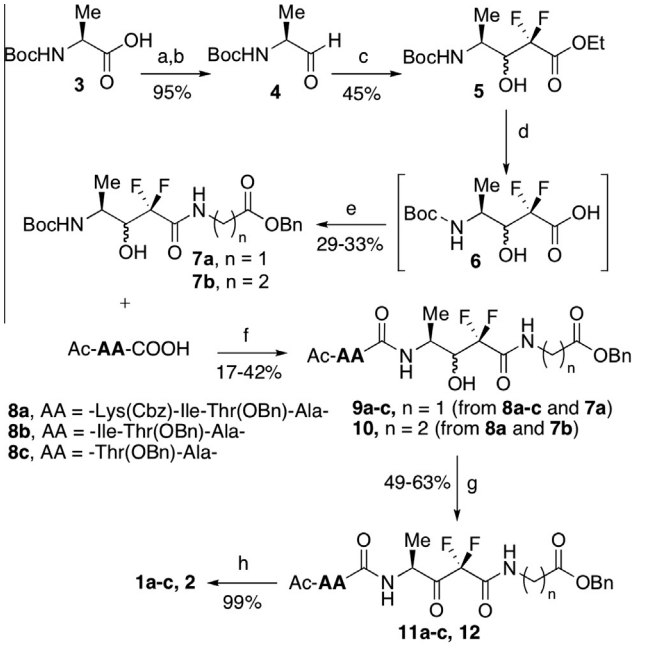

Scheme 2. Synthesis of difluorostatones **1a–c** and **2**. Reagents and conditions: (a) *N*,*O*-dimethylhydroxylamine hydrochloride, EDC, HOBt, DIPEA, dry DCM, 0–25 °C, 17 h; (b) $LiAlH_4$, dry THF, 0 °C, 20 min; (c) ethyl bromodifluoroacetate, zinc dust, dry THF, from 25 °C to reflux, 30 min; (d) 0.25 N solution of LiOH, MeCN, 25 °C, 2 h; (e) H-Gly-OBn·HCl (for **7a**) or H-βAla-OBn·HCl (for **7b**), HATU, DIPEA, dry THF, from 0 to 25 °C, 14 h; (f) (i) **7a**, **b**, TFA/DCM, 25 °C, 2 h, (ii) **8a–c**, EDC, HOBt, TEA, dry DMF, 0–25 °C, 12 h; (g) Dess–Martin periodinane, anhydrous NMP, from 0 to 25 °C, 1–24 h; (h) Pd/C 10%, H_2, 40 °C, 12–48 h.

of LiOH and the free carboxylic acid was immediately coupled to glycine or β-alanine benzyl esters in the presence of *O*-(7-azabenzotriazol-1-yl)-*N*,*N*,*N*′,*N*′-tetramethyluronium hexafluorophosphate (HATU) and *N*,*N*-diisopropylethylamine (DIPEA) in dry *N*,*N*-dimethylformamide (DMF) to afford the desired difluorostatine synthons **7a**, **b**. In the following steps of the synthetic pathway, statine-derivatives **7a**, **b** were exposed to a 50:50 mixture of trifluoroacetic acid (TFA) and dichloromethane (DCM) resulting in Boc-deprotection and formation of the corresponding trifluoroacetate salts. These latter compounds were immediately coupled with peptides **8a–c** using EDC and HOBt as coupling agents in dry DMF. Peptides **8a–c** were prepared by means of microwave assisted solid phase synthesis as described in the Supplementary data. Oxidation of the resulting alcohols **9a–c** and **10** with Dess–Martin periodinane in anhydrous *N*-methyl-2-pyrrolidone afforded difluorostatones **11a–c** and **12** in good yields.[19] Deprotection of the benzyl groups was accomplished using Pd/C in a hydrogen atmosphere (1 atm) providing the final compounds **1a–c** and **2** in quantitative yields.

The inhibitory activity of the synthesized inhibitors and selected intermediates against recombinant PfSUB1 (Table 1) was assessed using a previously described fluorimetric assay.[13] The design strategy of inhibitors, performed using a homology model of PfSUB1 built adopting a multiple template-based homology modeling approach, is reported in the Supporting information (Figs. S1–S13).[13,16,20,21]

Since the crystal structure of the PfSUB1 catalytic core (PDB ID: 4LVN[15]) is now available, we compared it to our previously developed homology model. The superposition depicted in Figure 1 reveals the good quality of the developed PfSUB1 homology model and validates our rational design approach. The sole difference observed in the two models (Fig. 1) is the side-chain orientation of Y427, which establishes an H-bond with K465 in the experimental structure.

Table 1
Percent inhibition of synthesized inhibitors against PfSUB1 at 100 μM. For inhibitors displaying >50% activity, the IC_{50} value is also reported

Structure	% Inhibit.	IC_{50} (μM)
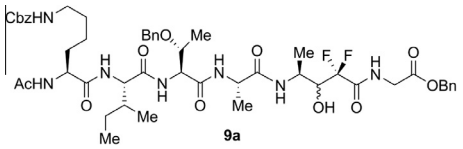 **9a**	3	–
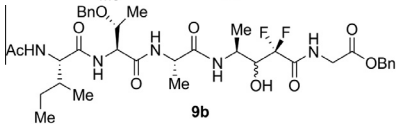 **9b**	0	–
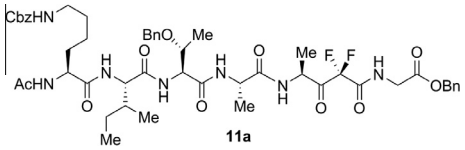 **11a**	71	5.0
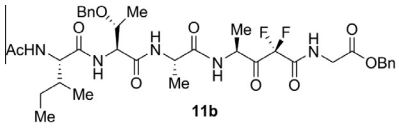 **11b**	59	33
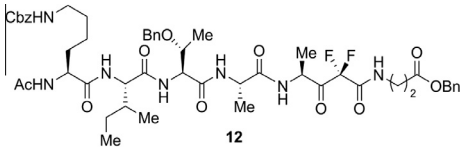 **12**	14	–
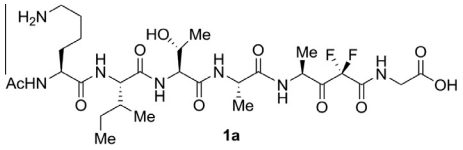 **1a**	100	0.6
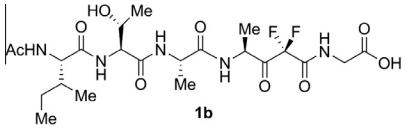 **1b**	99	0.6
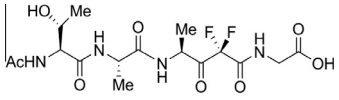 **1c**	6	–
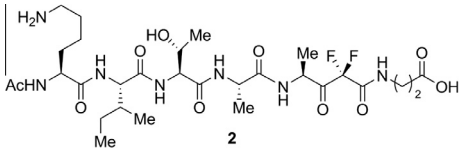 **2**	63	60

The reliability of our studies performed with PfSUB1 homology model, and the output obtained for the developed inhibitors (see Supplementary data) were also evaluated by means of docking studies (GOLD software[22]) performed on the crystal structure of PfSUB1. As expected, the binding poses found for all compounds analyzed and herein reported are in perfect agreement with the results obtained by the docking studies on the homology model.

The output of docking protocol for **1a** into the PfSUB1 crystal structure is depicted in Figure 2.

In the binding cleft of PfSUB1, **1a** maintains a series of interactions with key residues of the enzyme already observed as crucial for the binding of the crystallized substrate.[15] In particular, **1a** is engaged in H-bonding with S492, S519, G467, and H428, while K465 is engaged in a H-bond interaction with the difluorostatone amidic carbonyl. The free acidic function of **1a** establishes a series of H-bonds with R600, Y427 and K465. The formation of these polar contacts, along with **1a** favorable binding conformation, account for its very high binding score (93.56) with respect to the score found for the SERA4st1 (76.89, Fig. S1). Since docking score is not predictive in terms of the binding affinity, this latter was calculated by the estimation of the free-binding energy (ΔG_{bind}) by means of Prime MM/GBSA[23] using the docked pose belonging to the most populated cluster (Fig. 2). The calculated ΔG_{bind} of −127.54 kcal/mol revealed the high affinity of **1a** for the PfSUB1.

The same docking protocol using the crystal structure of PfSUB1 core was applied to inhibitor **2**, bearing a longer linker between the carboxylic acid and the difluorostatone moiety. As reported in Figure 3, compound **2** is not able to reproduce the strong pattern of interaction found for **1a**. Indeed, only the central portion of inhibitor **2** establishes H-bonds with K465 and S492. Both the Goldscore rate (75.41) and ΔG_{bind} value of −81.12 kcal/mol, confirm the lower affinity of **2** than **1a** for PfSUB1.

Please cite this article in press as: Giovani, S.; et al. *Bioorg. Med. Chem. Lett.* (2014), http://dx.doi.org/10.1016/j.bmcl.2014.05.044

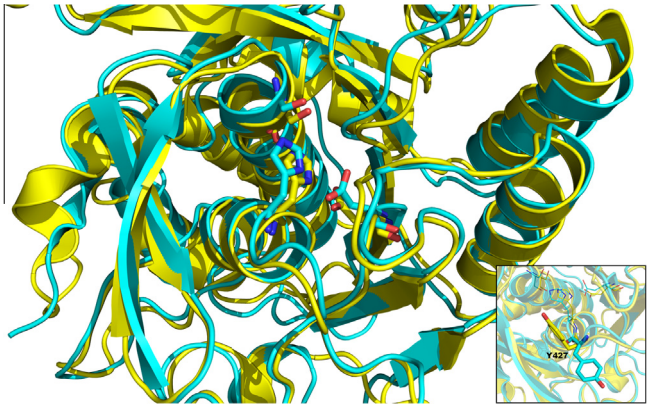

Figure 1. Superposition between the catalytic cleft of PfSUB1 obtained by homology modeling procedure (cyan cartoon) and of PfSUB1 crystal structure (yellow cartoon; PDB ID: 4LVN). The catalytic triad (S606, H428, D372) is represented by sticks. At the right bottom of the picture is highlighted the difference between the orientation found for Y427 in the homology model (cyan sticks) and in the crystal structure of PfSUB1 (yellow sticks). Molecular graphics were generated by PyMOL. Hydrogens were removed for the sake of clarity.

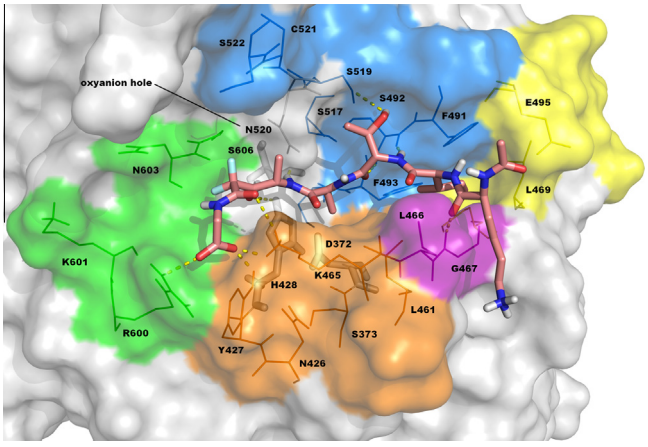

Figure 2. Docked pose of **1a** (light pink sticks) in the cavity of the PfSUB1 (PDB ID: 4LVN). H-bonds are indicated by yellow dotted lines. Molecular graphics were generated by PyMOL. Nonpolar hydrogens were omitted for clarity.

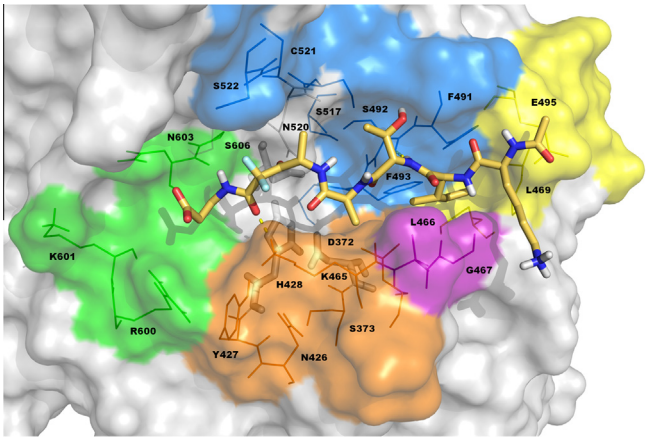

Figure 3. Docked pose of **2** (light yellow sticks) in the cavity of the PfSUB1 (PDB ID: 4LVN). H-bonds are indicated by yellow dotted lines. Molecular graphics were generated by PyMOL. Nonpolar hydrogens were omitted for clarity.

A notable difference between the binding mode of **1a** and **2** is the distance of the electrophilic carbon of the difluorostatone moiety from the catalytic S606 (Figs. S5 and S9), which is 5.0 Å for **1a** and 8.6 Å for **2**. Since difluorostatone is known to be a transition-state analogue, the distance of 5.0 Å displayed for **1a** from S606 is critical for an inhibitor/active site correct interaction. In fact difluorostatones inhibit serine proteases through a mechanism in which the electrophilic carbonyl group of the difluorostatone moiety, activated by the electron-withdrawing fluorine atoms, undergoes a nucleophilic attack by the active site serine forming a hemiketal tetrahedral intermediate.[24,25] In our series of inhibitors, this mechanism is also confirmed by the lack of activity at 100 μM of the statine-derivatives **9a**, **b** (**11a** vs **9a** and **11b** vs **9b** in Table 1).

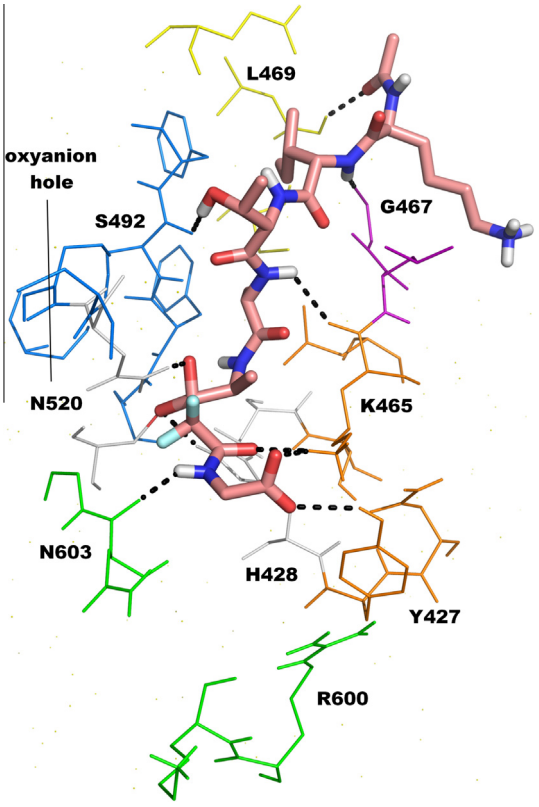

Figure 4. Minimized tetrahedral complex of PfSUB1/**1a** (light pink sticks). H-bonds are indicated by yellow dotted lines. The active site of PfSUB1 is represented by lines. Nonpolar hydrogens were removed for the sake of clarity.

To gain insight into the formation of the tetrahedral intermediate for predicting the binding mode of **1a**, a molecular model of the PfSUB1/**1a** tetrahedral complex was generated using a covalent docking protocol (GOLD).[26–29] As shown in Figure S9, a semiempirical calculation of ESP charge distribution confirmed that the C5 of **1a** is more electrophilic, and so more susceptible to nucleophilic attack from the oxygen of S606. The docked pose of **1a** into the catalytic site of PfSUB1 crystal structure was chosen as the starting point for the covalent docking procedure. As shown in Figure 4, the tetrahedral intermediate is stabilized by the formation of novel H-bond interactions with specific amino acid residues, thus resulting in an overall fine-tuning of the binding conformation of **1a** within the binding cleft and in the generation of a more stable complex. Comparing the binding poses of **1a** after the docking protocol (Fig. 2) and in the covalent docking simulation (Fig. 4), the lack of an H-bond with R600 and the formation of a new contact with N603 at the P′-side of **1a** is evident, due to a deeper incorporation of **1a** into the catalytic site. Instead, the contact of **1a** with H428 is maintained during covalent docking simulation.

Residues at the P-side of **1a** form strong H-bonds with K465 and S492. The most important contacts are found within the difluorostatone moiety, in particular those formed by the hemiketal oxygen with the oxyanion hole residue N520. A similar pattern of H-bond

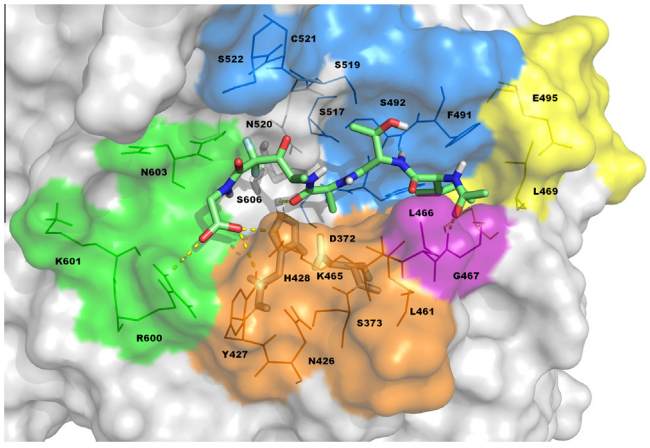

Figure 5. Docked pose of **1b** (light green sticks) in the cavity of the PfSUB1 (PDB ID: 4LVN). H-bonds are indicated by yellow dotted lines. Molecular graphics were generated by PyMOL. Nonpolar hydrogens were omitted for clarity.

contacts is known as essential for the stabilization of the tetrahedral intermediate within the serine protease catalytic site.[30] Our models of interaction clearly suggested that the P-side N-terminal lysine moiety of both the natural substrate (Fig. S1) and of inhibitor **1a** (Fig. 1) are not engaged in specific interactions with the enzyme. This led us to speculate that removal of this lysine residue from **1a**, thus generating **1b**, could be tolerated in terms of inhibitor potency. Inhibitor **1b** showed an inhibitory potency very similar to that of **1a** (Table 1), in agreement with its docking output (Fig. 5) showing a similar pattern of interaction with respect to **1a** (H-bonds with R600, Y427, K465, H428, S492, and G467) and also a comparable Goldscore (88.19) as well as the ΔG_{bind} (−119.10 kcal/mol). As expected, removal of the N-terminal lysine-isoleucine dipeptide (**1c**) abolished inhibitory activity (Table 1).

Compounds **1a**,**b** did not show activity against the mammalian proteases trypsin and chymotrypsin, while inhibitor **1a** showed good potency against the bacterial subtilisin Carlsberg protease (IC_{50} = 0.3 μM) thus indicating an interesting selectivity of these inhibitors for parasite over mammalian proteases. Experiments on the effect of inhibitors **1a**,**b** on schizont egress are in progress and will be communicated in due course.

In conclusion, we have successfully developed a novel series of potent peptidyl PfSUB1 inhibitors bearing a difluorostatone moiety as transition-state mimetic. Compounds **1a**,**b** are among the most potent and selective inhibitors of PfSUB1 reported in the literature. A sound homology model of PfSUB1 was generated and compared with the crystal structure of the enzyme. Our studies will pave the way to the next optimization of peptidomimetics to confirm PfSUB1 as a target for the development of innovative antimalarial agents.

Acknowledgments

The authors thank MIUR (PRIN) for financial support. M.P. was funded by the EU FP7-funded Marie Curie ITN STARS (contract number PITN-GA-2009-238490).

Supplementary data

Supplementary data associated with this article can be found, in the online version, at http://dx.doi.org/10.1016/j.bmcl.2014.05.044.

References and notes

1. Sonin, D. L.; Wakatsuki, T.; Routhu, K. V.; Harmann, L. M.; Petersen, M.; Meyer, J.; Strande, J. L. *J. Cardiovasc. Pharmacol. Ther.* **2013**, *18*, 460.
2. Gemma, S.; Travagli, V.; Savini, L.; Novellino, E.; Campiani, G.; Butini, S. *Recent Pat. Antiinfect. Drug Discovery* **2010**, *5*, 195.
3. Edwards, G.; Biagini, G. A. *Br. J. Clin. Pharmacol.* **2006**, *61*, 690.
4. Dondorp, A. M.; Nosten, F.; Yi, P.; Das, D.; Phyo, A. P.; Tarning, J.; Lwin, K. M.; Ariey, F.; Hanpithakpong, W.; Lee, S. J.; Ringwald, P.; Silamut, K.; Imwong, M.; Chotivanich, K.; Lim, P.; Herdman, T.; An, S. S.; Yeung, S.; Singhasivanon, P.; Day, N. P.; Lindegardh, N.; Socheat, D.; White, N. J.; Engl, N. *J. Med.* **2009**, *361*, 455.
5. Enserink, M. *Science* **2010**, *328*, 846.
6. Mousa, S. A. *Methods Mol. Biol.* **2010**, *663*, 157.
7. Wyles, D. L. *J. Infect. Dis.* **2013**, *207*, S33.
8. Blackman, M. J. *Cell. Microbiol.* **2008**, *10*, 1925.
9. Koussis, K.; Withers-Martinez, C.; Yeoh, S.; Child, M.; Hackett, F.; Knuepfer, E.; Juliano, L.; Woehlbier, U.; Bujard, H.; Blackman, M. J. *EMBO J.* **2009**, *28*, 725.
10. Yeoh, S.; O'Donnell, R. A.; Koussis, K.; Dluzewski, A. R.; Ansell, K. H.; Osborne, S. A.; Hackett, F.; Withers-Martinez, C.; Mitchell, G. H.; Bannister, L. H.; Bryans, J. S.; Kettleborough, C. A.; Blackman, M. J. *Cell* **2007**, *131*, 1072.
11. Collins, C. R.; Hackett, F.; Strath, M.; Penzo, M.; Withers-Martinez, C.; Baker, D. A.; Blackman, M. J. *PLoS Pathog.* **2013**, *9*, e1003344.
12. Gemma, S.; Giovani, S.; Brindisi, M.; Tripaldi, P.; Brogi, S.; Savini, L.; Fiorini, I.; Novellino, E.; Butini, S.; Campiani, G.; Penzo, M.; Blackman, M. J. *Bioorg. Med. Chem. Lett.* **2012**, *22*, 5317.
13. Withers-Martinez, C.; Suarez, C.; Fulle, S.; Kher, S.; Penzo, M.; Ebejer, J. P.; Koussis, K.; Hackett, F.; Jirgensons, A.; Finn, P.; Blackman, M. J. *Int. J. Parasitol.* **2012**, *42*, 597.
14. Arastu-Kapur, S.; Ponder, E. L.; Fonovic, U. P.; Yeoh, S.; Yuan, F.; Fonovic, M.; Grainger, M.; Phillips, C. I.; Powers, J. C.; Bogyo, M. *Nat. Chem. Biol.* **2008**, *4*, 203.
15. Withers-Martinez, C.; Strath, M.; Hackett, F.; Haire, L. F.; Howell, S. A.; Walker, P. A.; Evangelos, C.; Dodson, G. G.; Blackman, M. J. *Nat. Commun.* **2014**, 5. http://dx.doi.org/10.1038/ncomms4726.
16. Fulle, S.; Withers-Martinez, C.; Blackman, M. J.; Morris, G. M.; Finn, P. W. *J. Chem. Inf. Model.* **2013**, *53*, 573.
17. Fehrentz, J.-A.; Castro, B. *Synthesis* **1983**, *1983*, 676.
18. Wolfe, M. S.; Citron, M.; Diehl, T. S.; Xia, W.; Donkor, I. O.; Selkoe, D. J. *J. Med. Chem.* **1998**, *41*, 6.
19. Moore, C. L.; Leatherwood, D. D.; Diehl, T. S.; Selkoe, D. J.; Wolfe, M. S. *J. Med. Chem.* **2000**, *43*, 3434.
20. Cappelli, A.; Manini, M.; Valenti, S.; Castriconi, F.; Giuliani, G.; Anzini, M.; Brogi, S.; Butini, S.; Gemma, S.; Campiani, G.; Giorgi, G.; Mennuni, L.; Lanza, M.; Giordani, A.; Caselli, G.; Letari, O.; Makovec, F. *Eur. J. Med. Chem.* **2013**, *63*, 85.
21. Gemma, S.; Camodeca, C.; Brindisi, M.; Brogi, S.; Kukreja, G.; Kunjir, S.; Gabellieri, E.; Lucantoni, L.; Habluetzel, A.; Taramelli, D.; Basilico, N.; Gualdani, R.; Tadini-Buoninsegni, F.; Bartolommei, G.; Moncelli, M. R.; Martin, R. E.; Summers, R. L.; Lamponi, S.; Savini, L.; Fiorini, I.; Valoti, M.; Novellino, E.; Campiani, G.; Butini, S. *J. Med. Chem.* **2012**, *55*, 10387.
22. Jones, G.; Willett, P.; Glen, R. C. *J. Mol. Biol.* **1995**, *245*, 43.
23. Prime, version 3.0, Schrödinger, LLC, New York, NY, 2011.
24. Imperiali, B.; Abeles, R. H. *Biochemistry* **1986**, *25*, 3760.
25. Takahashi, L. H.; Radhakrishnan, R.; Rosenfield, R. E.; Meyer, E. F.; Trainor, D. A. *J. Am. Chem. Soc.* **1989**, *111*, 3368.
26. Ouyang, X.; Zhou, S.; Su, C. T.; Ge, Z.; Li, R.; Kwoh, C. K. *J. Comput. Chem.* **2013**, *34*, 326.
27. Soh, B. Y.; Song, H. O.; Lee, Y.; Lee, J.; Kaewintajuk, K.; Lee, B.; Choi, Y. Y.; Cho, J. H.; Choi, S.; Park, H. *Malar. J.* **2013**, *12*, 47.
28. Ghosh, A. K.; Gong, G.; Grum-Tokars, V.; Mulhearn, D. C.; Baker, S. C.; Coughlin, M.; Prabhakar, B. S.; Sleeman, K.; Johnson, M. E.; Mesecar, A. D. *Bioorg. Med. Chem. Lett.* **2008**, *18*, 5684.
29. Wang, Q.; Mach, R. H.; Reichert, D. E. *J. Chem. Inf. Model.* **2009**, *49*, 1963.
30. Robertus, J. D.; Kraut, J.; Alden, R. A.; Birktoft, J. J. *Biochemistry* **1972**, *11*, 4293.